

## Nanostructures fabrication by template deposition into anodic alumina membranes

R. Inguanta, G. Ferrara, S. Piazza, C. Sunseri

Dipartimento di Ingegneria Chimica dei Processi e dei Materiali  
Università di Palermo, Viale delle Scienze, 90128 Palermo (Italy)

In recent years, nanostructured materials have attracted growing interest due to their specific properties, which allow application in several fields such as photonics, nanoelectronics, thermoelectronics (Kelsall et al., 2005). For the fabrication of nanostructures, different methods have been proposed. Template synthesis is extremely interesting due to its simplicity and versatility (Martin, 1996). A variety of materials including metals, oxides, conductive polymers, and semiconductors can be deposited within the pores of either polycarbonate or anodic alumina membranes (AAM). The deposition process produces nanotubes (NTs), nanowires (NWs), or nanorods, whose dimensions can be easily controlled by adjusting template pore geometry and deposition conditions (Inguanta et al., 2007a).

In this work, different nanostructures of metals (Ni, Cu and Pd), alloys (Co-Sn), and metal oxides ( $\text{Cu}_2\text{O}$ ,  $\text{CeO}_2$ ,  $\text{PbO}_2$ ) have been fabricated, by electrochemical methods (electroless deposition, electrodeposition and displacement deposition), using AAM as template. Ni electroless deposition resulted in the formation of short metal nanotubes (about 5  $\mu\text{m}$  long). Different results were obtained by Ni electrodeposition, performed applying unipolar pulsed voltage perturbations. With a triangular wave, we have fabricated ordered arrays of metal nanowires, whilst with a square perturbation Ni nanotubes were produced. By electrochemical deposition, amorphous Sn-Co nanowires were also obtained. Co content in the alloy, length and crystallographic structure of nanowires varied with the deposition time.

Large arrays of aligned copper(I) oxide nanowires were, also, produced by electrodeposition. Two fundamental parameters were studied: potential perturbation and bath composition. We have found that these parameters influence both composition and crystallographic nature of  $\text{Cu}_2\text{O}$  nanowires. The electrochemical route was also used to fabricate  $\text{CeO}_2$  nanotubes from a non-aqueous electrolyte. The results, obtained by Raman spectroscopy, demonstrate that  $\text{CeO}_2$  nanotubes are suitable for catalytic applications.  $\text{PbO}_2$  nanowires having high aspect ratios were grown by potentiostatic electrodeposition under anodic polarization. Different electrolytic solutions were used in order to obtain nanowires of pure  $\alpha$ - $\text{PbO}_2$ , pure  $\beta$ - $\text{PbO}_2$ , or an  $\alpha + \beta$  mixture. In all deposition conditions, perfectly cylindrical wires, having uniform diameters throughout length were obtained. In this paper we describe also a novel method for the fabrication of a regular and uniform array of metal nanowires into anodic alumina membranes. The method is based on the metal displacement deposition realized into template pores by using a special arrangement, properly designed in order to optimize the processes.

## 1. Experimental Details

Nanostructured materials were grown into the pores of commercially available AAM (Whatman, Anodisc 47) having an average pore diameter of about 210 nm. The method of electrode preparation was detailed in previous works (Inguanta et al., 2007b, 2008b). Electrochemical experiments were performed using P.A.R. Potentiostat/Galvanostat (mod. 273A and 2273) connected to a desk computer for data acquisition and control. A standard three-electrode cell was employed, having a graphite sheet and a saturated calomel electrode (SCE) as counter and reference electrodes, respectively. Length of nanostructures was controlled by adjusting the electrodeposition time. Chemical composition and morphology of nanostructures were investigated by SEM, EDS, XRD and RAMAN spectroscopy. These characterization methods are detailed elsewhere (Inguanta et al., 2007b-c).

## 2. Results and Discussion

### 2.1 Metal and Alloy Nanostructures

In order to fabricate Ni NTs, nickel electroless deposition was performed from a bath containing Ni sulphate according to the procedure reported in a previous work (Inguanta et al., 2007a). EDS analysis revealed that NTs contain mainly Ni and P, with small amounts of others elements coming from the deposition bath. The presence of P into the deposited metallic layer was confirmed by XRD patterns, showing peaks relative to Ni, Ni<sub>3</sub>P and Ni<sub>3</sub>P<sub>2</sub>, and it is due to the sodium hypophosphite used as reducing agent. The structure of nanotubes (length of about 5  $\mu$ m) is well evidenced in Fig. 1a, obtained after dissolution of the AAM template in 1 M NaOH solution.

Better results were achieved by electrodeposition from a Watt bath (containing Ni sulphate, Ni chloride and boric acid at pH 4.5) by applying a unipolar pulsed voltage perturbation between 0 and -3 V(SCE) at room temperature (Inguanta et al., 2008c). In particular, it was found that the shape of nanostructures depends on the potential waveform. Under a square potential waveform, nanotubes of Ni were fabricated inside the channels of AAM (Fig. 1b). Up to 30 minutes of deposition, nearly cylindrical nanotubes were formed. For longer times, the inner shape of nanotubes evolved from cylindrical to conical, due to the progressive shutting of the bottom. Under a trapezoidal wave, Ni nanowires were formed (Fig. 1c), whose length increased with deposition time. Their growth rate was constant up to 60 minutes of deposition, whilst for longer times non-uniform lengths were observed in different channels. The formation of different nanostructures (either nanowires or nanotubes) and the modification of the inner shape of nanotubes with increasing the deposition time were explained by invoking the screening effect by hydrogen bubbles that are formed simultaneously to Ni deposition. In the case of trapezoidal waveform, small bubbles of hydrogen are formed leaving sufficient free surface for deposition of Ni, which consequently occurs over the entire inner surface of the channels. On the contrary, a square potential pulse leads to the formation of bigger gas bubbles, that screen the bottom surface of pores; thus, the deposition of Ni is confined into the gap between bubbles and channel wall.

By electrochemical deposition, amorphous Sn-Co nanowires were also obtained. The deposition was performed at -1.0 V(SCE) and 60 °C in a solution of 0.005 M CoSO<sub>4</sub> and 0.01 M SnSO<sub>4</sub> in the presence of 0.2 M Na<sub>2</sub>SO<sub>4</sub> (supporting electrolyte) and 0.2 M of sodium gluconate (as chelating agent) (Ferrara et al., 2008a,b). Alloys deposited for 15÷60 min were amorphous, whilst after 90 min some XRD peaks appeared, but their intensity was so weak that we can consider amorphous the alloys also for these

conditions of preparation. By adjusting the deposition time, NWs of different composition and length were formed. The content of Co in the alloy varied from less than 38 at%, after 10 min of deposition, to about 44 at%, after 90 min. The change in the composition of the alloy seems to influence also its rate of deposition, which increases with the content of Co in the alloy. The length of the NWs changed from less than 2  $\mu\text{m}$ , after 10 min, to about 16  $\mu\text{m}$ , after 90 min. For short deposition times, length of NWs was uniform (Fig. 1d), whilst after 90 min slightly different lengths were observed.

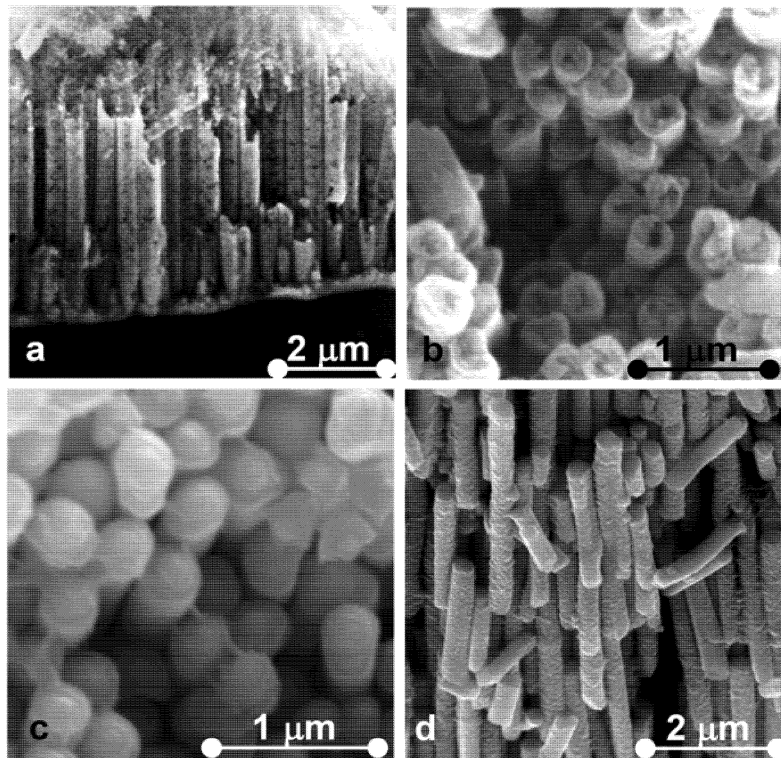


Figure 1. (a) Ni nanotubes obtained by electroless deposition; (b) Ni nanotubes and (c) Ni nanowires obtained by electrodeposition; (d) Sn-Co nanowires.

## 2.1 Metal Oxide Nanostructures

By template electrodeposition, we have obtained nanostructures of  $\text{Cu}_2\text{O}$ ,  $\text{CeO}_2$  and  $\text{PbO}_2$ . In order to obtain  $\text{Cu}_2\text{O}$  nanostructures, the electrodeposition was carried out by applying different potential perturbations (continuous and pulsed) at  $55^\circ\text{C}$ . For the potentiostatic deposition, a continuous electrode potential of  $-0.2\text{ V(SCE)}$  was applied, whilst for the unipolar pulsed electrodepositions, square and trapezoidal voltage perturbations were imposed. In this last case, potential was cycled between 0 and  $-0.2\text{ V(SCE)}$  for several runs. Two different electrolytic solutions were used: the first was a 0.01 M cupric acetate / 0.1 M sodium acetate bath at  $\text{pH}=6.5$ , whilst the second plating bath was prepared by dissolving 0.4 M  $\text{CuSO}_4$  in a 3 M lactic acid solution, with  $\text{pH}$  adjusted to 10 (Inguanta et al., 2008b). We have found that by potentiostatic

electrodeposition from the copper acetate bath, simultaneous deposition of copper oxide and copper metal occurred. This result, confirmed by XRD analysis, is likely due to a local decrease of pH close to the electrode/solution interface. SEM analysis showed that in this case the average NWs length was about 3.8  $\mu\text{m}$  after 3 hours of electrodeposition. The same bath produced pure  $\text{Cu}_2\text{O}$  NWs when unipolar pulsed electrodeposition was employed. In this latter case a better control of local pH was achieved, because during delay time at 0 V the initial conditions of pH close to electrodeposition interface are restored before next deposition pulse starts. XRD analysis revealed polycrystalline NWs with a cubic structure.

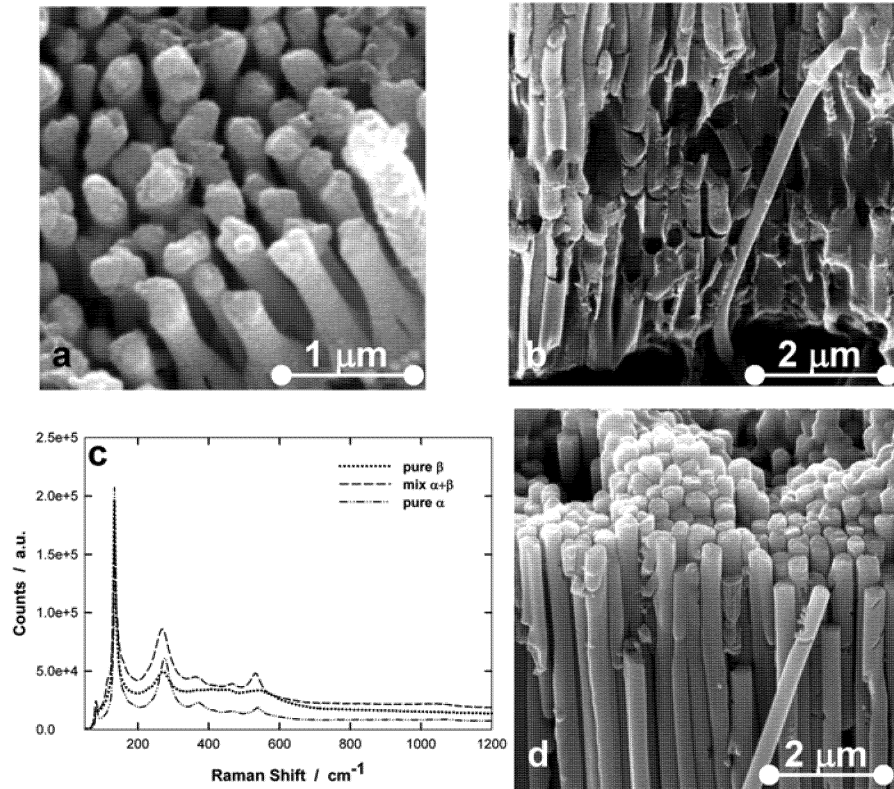


Figure 2. (a)  $\text{Cu}_2\text{O}$  nanowires; (b)  $\text{CeO}_2$  nanotubes; (c)  $\text{PbO}_2$  nanowires; (d) Raman spectra of  $\text{PbO}_2$  nanowires.

In the copper lactate bath, pure copper oxide was deposited even under potentiostatic polarization, and for both continuous and pulsed voltage perturbations polycrystalline NWs with a strong preferential orientation along the (200) plane were obtained. They presented a high crystalline order degree, with an average grain size of about 42 nm. In both solutions, NWs present the same morphology (Fig. 2a): a continuous and dense array of cylindrical wires, having a diameter of about 200 nm, throughout the length.  $\text{Cu}_2\text{O}$  NWs were uniformly distributed in all channels of the membrane, and their population density was of the order of  $10^{13} \text{ m}^{-2}$ . These arrays, display both anodic and

cathodic photocurrent, with a sign inversion dependent on wavelength, potential, and nanowire length (Inguanta et al., 2007d).

By potentiostatic deposition from an organic solution, we have obtained nanotubes of CeO<sub>2</sub> (Inguanta et al., 2007b). The composition of the plating solution was 0.3 M CeCl<sub>3</sub>•7H<sub>2</sub>O in absolute ethyl alcohol and the electrodeposition was performed at -10 V(SCE) at room temperature. Nanotubes had somewhat uniform diameters, with an average external value of about 210 nm, and a maximum length of about 60 μm; the latter parameter was controlled by the electrodeposition time (Fig. 2b). Each single nanotube was found to consist of crystalline grains having a size of about 3 nm. The presence of the vibrational band at 600 cm<sup>-1</sup> in the Raman spectrum suggests that ceria NTs are suitable for application in catalytic reactions.

The electrochemical route was also used to fabricate large arrays of PbO<sub>2</sub> nanowires having high aspect ratios (Inguanta et al., 2008d). The electrodeposition was carried out at 1.5 V(SCE) and 60°C. Different electrolytic solutions were used in order to obtain nanowires of pure α-PbO<sub>2</sub>, pure β-PbO<sub>2</sub> and an α+β mixture; phases were identified by XRD and RAMAN analyses (Fig. 2c). We have found that in lead nitrate bath the crystallographic structure of nanowires depends on pH; this latter was varied adding diluted nitric acid to the electrolyte. Nanowires of pure β-PbO<sub>2</sub> were obtained at pH 0.6, whilst mixed α-PbO<sub>2</sub>+β-PbO<sub>2</sub> nanowires were grown at pH 2. Pure α-phase was obtained in a bath containing lead acetate at pH 6.6. In all deposition conditions, nanowires show the same morphology: perfectly cylindrical wires having uniform diameter throughout length (Fig. 2d). Length, and consequently the aspect ratio of PbO<sub>2</sub> NWs, increased with the electrodeposition time.

### 2.3 Metal Nanostructures by displacement deposition

We have recently proposed a novel route for fabricating metal nanowires (Inguanta et al., 2007c, 2008a). Here, we show some results relative to the growth of crystalline copper and palladium nanowires. The procedure is based on metal displacement reaction (Pauvonic and Schlesinger, 2000) (cementation of copper ions) leading to the growth of copper nanowires into the pores of commercially available alumina membranes. The galvanic displacement reaction for the synthesis of core/sheet nanostructured materials have been investigated in the literature (Sun et al., 2002). The key step of the proposed approach is the use of nanostructured materials as template and suitable salt precursor solution. On the contrary, we have obtained the direct growth of metal nanowires by the immersion of coupled different metals into an electrolytic solution containing metal ions. The displacement reaction was forced to occur within template pores, owing to the electrical contact between the two metals at pore bottom realized in our special arrangement. This technique of fabrication is very easy to control and cheap, because the cost of materials and necessary equipment for the process is very low. A further advantage of this approach, in comparison with other technologies, is the possibility to fabricate metal nanowires by using a very large area template. Besides, since this procedure is only dependent on the difference between the standard potentials of the two metals coupled, many other metallic nanowires could be prepared. A scheme of the arrangement used for the fabrication of metal nanowires is reported in our previous work (Inguanta et al., 2008a). Using this arrangement we have fabricated

regular and uniform arrays of Cu and Pd nanowires by displacement deposition process at room temperature. For the preparation of Cu NWs, a 0.2 M copper sulphate solution was used, while a solution containing  $\text{Pd}(\text{NH}_3)_4(\text{NO}_3)_2$  was employed for the fabrication of Pd NWs. The length of nanowires can be easily controlled by adjusting the immersion time in the electrolytic solution. SEM pictures showed the formation of perfectly aligned nanowires with high aspect ratio. Nanowires are straight, dense and continuous with a uniform diameter throughout the entire length (Fig. 2a-b). In all samples, length of the wires was uniform along the AAM cross-section. This finding indicates that nanowires grow at the same rate in each pore during the displacement deposition. XRD analysis revealed the formation of polycrystalline copper and palladium nanowires.

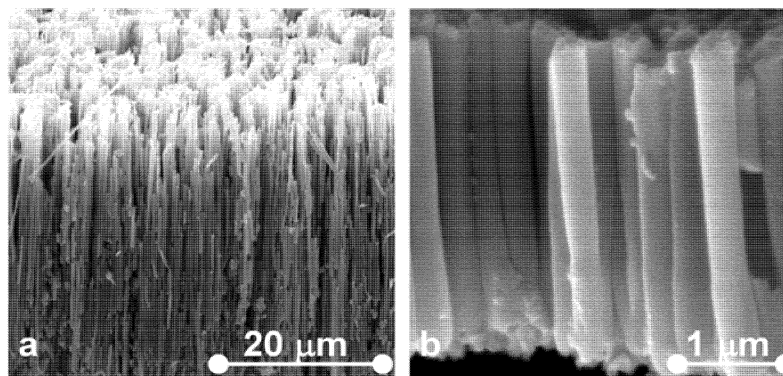


Figure 3. Copper (a) and palladium nanowires (b) obtained by displacement deposition.

Acknowledgments – This work is supported financially by University of Palermo – APQ Ricerca della Regione Siciliana delibera CIPE n° 17/2003. “Laboratorio dell’innovazione nel settore dei Beni Culturali: Sperimentazione di nanotecnologie e nanomateriali”.

### 3. References

- Ferrara G., Inguanta R., Piazza S., Sunseri C., 2008a, *Advanced Batteries and Accumulators*, Eds. Jiri Vondrak, Jiri Vognar, Timeart, Brno.
- Ferrara G., Inguanta R., Piazza S., Sunseri C., 2008b, Patent, RM2008A000341.
- Inguanta R., Butera M., Sunseri C., Piazza S., 2007a, *Appl. Surf. Sci.* 253, 5447.
- Inguanta R., Piazza S., Sunseri C., 2007b, *Nanotechnology*, 18, 561.
- Inguanta R., Piazza S., Sunseri C., 2007c, Patent, I.P. VI2007A000275.
- Inguanta R., Sunseri C., Piazza S., 2007d, *Electrochem. Solid-State Lett.* 10, K63.
- Inguanta R., Piazza S., Sunseri C., 2008a, *Electrochem. Comm.*, 10, 506.
- Inguanta R., Piazza S., Sunseri C., 2008b, *Electrochimica Acta*, 53, 6504.
- Inguanta R., Piazza S., Sunseri C., 2008c, *Electrochimica Acta*, 53, 5767.
- Inguanta R., Piazza S., Sunseri C., 2008d, *J. Electrochem. Soc.*, 155, K205.
- Kelsall R., Hamley I., 2005, *Nanoscale Science & Technology*. Wiley, Chichester.
- Martin C. R., 1996, *Chem. Mater.*, 8, 1739.
- Pauvonic M., Schlesinger M., 2000, *Modern Electroplating*, Wiley, New York.
- Sun Y., Mayers B. T., Xia Y., 2002, *Nano Lett.* 5, 481.